Computational Study on the Relative Acidity of Acetic Acid by the QM/MM Method Combined with the Theory of Energy Representation

Takumi Hori,[†,‡] Hideaki Takahashi,[*,†] Shin-ichi Furukawa,[†] Masayoshi Nakano,[†] and Weitao Yang[‡]

Division of Chemical Engineering, Department of Materials Engineering Science, Graduate School of Engineering Science, Osaka University, Machikaneyama-cho 1-3, Toyonaka, Osaka 560-8531, Japan, and Department of Chemistry, Duke University, Durham, North Carolina 27708

Received: September 26, 2006; In Final Form: November 13, 2006

We have applied the quantum mechanical/molecular mechanical (QM/MM) method combined with the theory of energy representation (ER) to study the acidity of acetic acid in aqueous solution. We have focused our attention on the relative acidity ΔpK_a of the molecule with respect to water solvent to circumvent the ambiguity of the solvation free energies of the molecular species referred to as *proton*. The value of ΔpK_a for the acetic acid has been computed as −11.5 when we adopt the free energy change in the gas phase obtained by the B3LYP functional, which is in excellent agreement with the experimental value of −11.0. It has been demonstrated that the QM/MM-ER approach recently developed gives an adequate description for the solvation free energies related to the acidity/basicity calculations of organic molecules.

I. Introduction

Protonation and deprotonation states of organic molecules have a great concern with the pH-dependent properties of chemical events in solution[1−11] and biological systems.[12−21] In organic chemistry, knowledge on the acidity/basicity of a solute molecule is the basis for understanding the reaction mechanism. As for biochemistry, ionizable amino acid residues often play key roles in fundamental processes like protein foldings, enzyme reactions, and substrate bindings. Since many chemical and physical processes in condensed systems are, thus, strongly influenced by the acidity of the chemically active sites, prediction of the protonation states by means of computational methodologies is attracting a great deal of attention in a variety of fields. Since the deprotonation of a solute involves a chemical bond dissociation, the quantum chemical approach is essential for the theoretical investigation. Moreover, ionic dissociation is substantially stabilized under the influence of the aqueous environment through the electrostatic interaction, hence the explicit consideration of the solvation effect of the water molecules is also required.

There have been several developments to incorporate the solvation effects in the quantum chemical calculations. The polarizable continuum model (PCM)[22] has been widely utilized to compute solvation free energies for many solution systems.[1,2] The notable advantage of the PCM approach is that the computational effort is reasonable since the solvent is modeled by a continuum of uniform dielectric constant. A critical drawback of the approximation is obviously that it cannot take into account the short range solute−solvent interaction such as hydrogen bonds. A more sophisticated approach to compute solvation free energy can be given by the reference-interaction-site model combined with the self-consistent field procedure (RISM-SCF),[3−8,23] where the molecular shape of the solvent is reduced to a set of the interaction sites placed on the solvent molecule. The solvation free energy of the solute is then expressed in terms of the site−site radial distribution functions which are obtained by a solution of the integral equations in combination with the SCF procedures for the wave function of the solute. However, its application is limited to high-density regions of solution and the point charge representation is not adequate to reproduce the electrostatic fields formed by anionic solutes.

A promising way to compute the electronic wave function of a solute in solution is to employ the hybrid quantum mechanical/molecular mechanical (QM/MM) approach,[24] where only the chemically active sites are treated by quantum mechanics, while the environment is described by classical molecular mechanics. It has been demonstrated by many works[9−11,17,25−33] that the QM/MM approach allows one to simulate the chemical events in condensed systems with substantial accuracy. However, it requires a large number of ensembles for the molecular configurations to attain the convergence in the free energy calculation. Therefore, the QM/MM simulation that employs the numerically rigorous approach[9−11,27−33] such as free energy perturbation or thermodynamic integration is still demanding even under a state-of-the-art computational environment.

To overcome such difficulties associated with the free energy calculation for the chemical event, Takahashi and Matubayasi recently developed a novel methodology (QM/MM-ER)[34] that combines the QM/MM approach[35−41] with the theory of energy representation (ER).[42−44] Within the conventional theory of solution, the excess chemical potential of a solute is determined by a spatial distribution function of the solvent around the solute or practically by its reduced form, i.e., a set of site−site radial distribution functions. In the theory of energy representation, on the other hand, the solvation free energy of a solute is described in terms of the distribution functions for the solute−solvent interaction energy. The application of the theory of

* Author to whom correspondence should be addressed. E-mail: takahasi@cheng.es.osaka-u.ac.jp.
† Osaka University.
‡ Duke University.

10.1021/jp066334d CCC: $37.00
Published on Web 01/03/2007

energy representation to a quantum chemical object, where the electrons are continuously distributed over the space, can be accomplished without the loss of accuracy since there is no need to employ a site−site form of interaction potential in the practical implementations. Some of the authors recently performed the QM/MM-ER simulations to address the issue of autoionization of a water molecule in aqueous solution[45] and found that the QM/MM-ER approach is efficient enough to reproduce the solvation free energies for neutral molecules showing excellent agreements with other theoretical results. We also applied the methodology to compute the free energy difference between the anti and syn conformations of the acetic acid in solution[46] and found that the QM/MM-ER approach is adequate enough to study a process that accompanies only slight free energy change.

In the present paper, we carry out the QM/MM-ER simulations aiming at the computation of the acidity or the basicity of organic molecules in solution. As a simple test, the free energy difference between the acetic acid and the acetate ion is computed to evaluate the relative acidity of the acetic acid with respect to H_2O. We focus our interest not on the pK_a value itself but on the relative acidity of the molecule since the determination of pK_a involves the problem of the solvation free energies of the molecular species categorized as proton (H_3O^+, $H_5O_2^+$, $H_7O_3^+$, ...). To circumvent the ambiguity of the *proton* solvation free energy, we discuss here the solvation free energies of the acetate or hydroxy anion in solution. The following section will be devoted to the derivation of the equation defining the relative acidity and the review of the QM/MM-ER methodology. The computational procedures for the QM/MM-ER simulations will be given in the Computational Details section. The efficiency and the accuracy of the present method will be discussed in the Results and Discussion.

II. Methodology

In the present section, we provide equations to describe the acidity of molecules in solution. First we introduce the concept of the relative acidity as a measure of the relative acid strength of an organic molecule with respect to water. Next, the relative acidity is expressed in terms of several kinds of free energies which can be obtained by the quantum chemical calculations in either the gas phase or solution. At the end of the section, we present a brief review of the QM/MM-ER approach,[34] which plays a central role in the determination of the relative acidity of a molecule in solution.

A. Relative Acidity of an Organic Molecule. A proton dissociation reaction of an organic molecule in water is described by the equation

$$AH + H_2O \leftrightarrow A^- + H_3O^+ \tag{1}$$

where AH represents a titratable organic molecule and A^- is the conjugate base of AH. As a special case where a water molecule is regarded as a reactant AH, eq 1 can be written as

$$2H_2O \leftrightarrow OH^- + H_3O^+ \tag{2}$$

Subtracting eq 2 from eq 1, we obtain the equation

$$OH^- + AH \leftrightarrow A^- + H_2O \tag{3}$$

This equation expresses the reaction between the acid molecule AH and the conjugate base of water (OH^-), hence its equilibrium constant can be regarded as a measure for the acid strength of AH relative to that of H_2O.

The equilibrium constant K_{AH/H_2O} for eq 3 is expressed by the equation

$$K_{AH/H_2O} = \frac{[A^-][H_2O]}{[AH][OH^-]} = \frac{V(AH)V(OH^-)}{V(A^-)V(H_2O)} \tag{4}$$

where the bracket denotes the molar concentration of the solute molecule in solution and the term V represents a mean volume for a solute molecule at the equilibrium state. Here, we define the relative acidity for the organic molecule by the negative logarithm of the equilibrium constant K_{AH/H_2O}, referred to as ΔpK_a. We note that ΔpK_a can also be expressed by the difference between the pK_a value of the organic molecule and that of water ($pK_a^{H_2O}$), thus,

$$\Delta pK_a = -\log K_{AH/H_2O} = pK_a^{AH} - pK_a^{H_2O} \tag{5}$$

As shown by eq 5, the larger positive value of ΔpK_a indicates that the molecule AH is weaker as an acid reagent as compared with water. The concept of the relative acidity also enables one to avoid the ambiguity of the solvation free energies for the species categorized as proton. In the next subsection, we consider the free energy components which are needed to compute relative acidity.

B. Free Energy Components in Chemical Potential. At the equilibrium of the reaction expressed by eq 3, the chemical potential μ for the reactant is equal to that for the product, namely,

$$\mu(OH^-) + \mu(AH) = \mu(A^-) + \mu(H_2O) \tag{6}$$

The chemical potential for the solute molecule X (=OH^-, AH, A^-, and H_2O) can be decomposed into the contributions

$$\mu(X) = \mu_{trans}(X) + E_0(X) + E_{ZPE}(X) + \mu_{vibrot}(X) + \mu_{solv}(X) + k_BT \ln[X] \tag{7}$$

where the terms in the right-hand side indicate in order the translational free energy, the electronic energy in the gas phase, the zero-point energy, the vibration−rotational free energy, and the solvation free energy for the solute X. The translational free energy μ_{trans} can be expressed by

$$\mu_{trans} = k_BT \ln(\lambda(X)) \tag{8}$$

where $\lambda(X)$ is the third power of the thermal de Broglie wave length, which can be written as

$$\lambda(X) = \left(\frac{h^2}{2\pi m_X k_B T}\right)^{3/2} \tag{9}$$

where m_X, k_B, T, and h are respectively the mass of the solute X, the Boltzmann constant, the temperature of the system, and Planck's constant. Substituting eq 7 and eq 8 into eq 6, one obtains

$$\ln\frac{[A^-][H_2O]}{[AH][OH^-]} = \ln\frac{\lambda(AH)\lambda(OH^-)}{\lambda(A^-)\lambda(H_2O)} - \frac{\Delta G_0}{k_BT} \tag{10}$$

where ΔG_0 is the difference of the sum of the free energy components between the final and the initial states except for the first and last term in eq 7, thus,

$$\Delta G_0 = \Delta E_0 + \Delta E_{ZPE} + \Delta\mu_{vibrot} + \Delta\mu_{solv} \tag{11}$$

A simple algebraic manipulation of eq 10 gives the relative acidity defined by eq 5 as follows,

$$\Delta \mathrm{p}K_a = -\frac{1}{2.303}\ln\left[\frac{\lambda(\mathrm{AH})\lambda(\mathrm{OH}^-)}{\lambda(\mathrm{A}^-)\lambda(\mathrm{H_2O})}\exp\left(-\frac{\Delta G_0}{k_B T}\right)\right] \quad (12)$$

The terms in eq 11 that constitute ΔG_0 can be computed by performing frequency analyses and the QM/MM-ER simulations. E_0 is given by the energy of the QM solute at the optimized geometry in the gas phase and the vibrational−rotational free energy μ_{vibrot} and the zero-point energy E_{ZPE} are also determined in the gas phase by frequency analyses in the Gaussian package.[47] The solvation free energy μ_{solv} can be obtained by the QM/MM-ER simulation,[34] which is computationally most demanding in the present work. In the following subsection, we briefly review the QM/MM-ER approach recently developed.

C. QM/MM-ER Approach. The total energy of the QM/MM system is typically given by

$$E = E_{\mathrm{QM}} + E_{\mathrm{QM/MM}} + E_{\mathrm{MM}} \quad (13)$$

where E_{QM} is the energy of the QM subsystem, $E_{\mathrm{QM/MM}}$ denotes the interaction between the QM and MM subsystem, and E_{MM} is the energy of the MM subsystem. By defining H_0 as the Hamiltonian of the QM solute at isolation including the nuclear−nuclear repulsion energy, E_{QM} in eq 13 is expressed by

$$E_{\mathrm{QM}} = \langle \Psi | H_0 | \Psi \rangle \quad (14)$$

where Ψ is the solution of the electronic Schrödinger equation for the QM subsystem under the influence of the electrostatic potential formed by MM molecules. Here, we introduce the distortion energy E_{dist} of the QM solute for the later reference, thus,

$$E_{\mathrm{dist}} = \langle \Psi | H_0 | \Psi \rangle - E_0 \quad (15)$$

where E_0 is the energy of the QM solute at isolation, i.e., eigenvalue of the Hamiltonian H_0. Note that E_{dist} is always positive in solution. $E_{\mathrm{QM/MM}}$ in eq 13 is dependent on the instantaneous electron density $n(\mathbf{r})$ of the QM solute as well as the solvent configuration and can be written as

$$E_{\mathrm{QM/MM}} = \sum_i v(n,\mathbf{x}_i) \quad (16)$$

where $\mathbf{x}_i$ stands for the full coordinate of the ith solvent molecule with respect to the solute.

Within the theory of energy representation,[34,42−44] the distribution functions for the solute−solvent interaction energy play an essential role to determine the excess chemical potential of a solute molecule. At first we define the instantaneous energy distribution function as

$$\hat{\rho}(\epsilon) = \sum_i \delta(v(\mathbf{x}_i) - \epsilon) \quad (17)$$

where the sum is taken over solvent molecules around the solute. In eq 17 the potential v is introduced to define the energy coordinate of a solvent molecule and usually taken as the two-body interaction potential of interest between the solute and the solvent. Then, the energy distribution function $\rho(\epsilon)$ is constructed through the ensemble average of the instantaneous distribution $\hat{\rho}(\epsilon)$ under the condition that the solute−solvent interaction is u, thus,

$$\rho_u(\epsilon) = \langle \hat{\rho}(\epsilon) \rangle_u = \frac{\int \mathrm{d}\mathbf{X}\hat{\rho}(\epsilon)\exp[-\beta(\sum_i u(\mathbf{x}_i) + U(\mathbf{X}))]}{\int \mathrm{d}\mathbf{X}\exp[-\beta(\sum_i u(\mathbf{x}_i) + U(\mathbf{X}))]} \quad (18)$$

where $\mathbf{X}$ expresses the set of the full coordinates $\{\mathbf{x}_i\}$ and $U(\mathbf{X})$ is the solvent−solvent interaction. In particular, when we take $u = 0$ in eq 18, the system is referred to as the reference system and the resulting energy distribution function is written as $\rho_0(\epsilon)$. On the other hand, when $u = v$ the system is referred to as the solution system and the energy distribution function is simply denoted as $\rho(\epsilon)$. In the reference system, the solute molecule is placed in the neat solvent as a test particle to construct the energy distribution function. Then, the solvation free energy $\Delta\mu$ of a solute is exactly expressed in terms of the energy distribution functions, thus,

$$\Delta\mu = -k_B T \int \mathrm{d}\epsilon[[\rho(\epsilon) - \rho_0(\epsilon)] + \beta\omega(\epsilon;1)\rho(\epsilon) - \beta(\int_0^1 \mathrm{d}\lambda\omega(\epsilon;\lambda))[\rho(\epsilon) - \rho_0(\epsilon)]] \quad (19)$$

where $\omega(\epsilon;\lambda)$ is the indirect part of the solute−solvent potential of mean force and λ is the coupling parameter associated with the gradual insertion of the solute. An approximate expression for the λ-integral of $\omega(\epsilon;\lambda)$ is formulated by adopting a hybrid functional of the Percus−Yevick (PY) and the hypernetted chain (HNC) forms.[43] The accuracy of the approximate functional has been well examined in previous work.[34,41,45,46]

Within the framework of the standard theory of energy representation,[42−44] the solute−solvent interaction potential is supposed to be pairwise additive. To take into account many-body effects inherent in the QM/MM potential, we divide the excess chemical potential μ_{solv} in eq 7 into three components,[34]

$$\mu_{\mathrm{solv}} = \Delta\bar{\mu} + \bar{E} + \delta\mu \quad (20)$$

$\Delta\bar{\mu}$ in eq 20 is the solvation free energy for the solute with the electron density fixed at its average distribution $\tilde{n}(\mathbf{r})$ in solution. $\tilde{n}(\mathbf{r})$is the statistical average of the electron density $n(\mathbf{r})$ and can be explicitly given by using the notations in eqs 15 and 16, thus,

$$\tilde{n}(\mathbf{r}) = \frac{\int \mathrm{d}\mathbf{X}n(\mathbf{r})\exp[-\beta(E_{\mathrm{dist}} + \sum_i v(n,\mathbf{x}_i) + U(\mathbf{X}))]}{\int \mathrm{d}\mathbf{X}\exp[-\beta(E_{\mathrm{dist}} + \sum_i v(n,\mathbf{x}_i) + U(\mathbf{X}))]} \quad (21)$$

Since the interaction potential for the solute with $\tilde{n}(\mathbf{r})$ is pairwise additive, eq 19 can be adopted straightforwardly to compute $\Delta\bar{\mu}$. $\bar{E}$ in eq 20 is the statistical average of the energy E_{dist} and can be expressed as

$$\bar{E} = \frac{\int \mathrm{d}\mathbf{X}E_{\mathrm{dist}}\exp[-\beta(E_{\mathrm{dist}} + \sum_i v(n,\mathbf{x}_i) + U(\mathbf{X}))]}{\int \mathrm{d}\mathbf{X}\exp[-\beta(E_{\mathrm{dist}} + \sum_i v(n,\mathbf{x}_i) + U(\mathbf{X}))]} \quad (22)$$

The last term $\delta\mu$ in eq 20 is the free energy due to the electron density fluctuation around the average distribution $\tilde{n}(\mathbf{r})$, which

TABLE 1: Lennard-Jones Parameters for the CH_3COOH and CH_3COO^- Molecules[a]

	CH_3COOH		CH_3COO^-	
	σ	ϵ	σ	ϵ
C1	3.500	0.066	3.500	0.066
H2, 3, 4	2.500	0.030	2.500	0.030
C2	3.750	0.105	2.636	0.105
O1	3.000	0.170	2.081	0.210
O2	2.960	0.210	2.081	0.210
H4	0.000	0.000	-	-

[a] σ and ϵ are in the units of Å and kcal/mol, respectively.

originates from the many-body effect of the QM solute. $\delta\mu$ can be obtained by performing additional QM/MM simulations.[34,41,45] It should be noted that $\Delta\bar{u}$ and $\bar{E}$ give the major contribution to the free energy difference between the reactant and the product in a chemical reaction and the remaining term $\delta\mu$ can be safely neglected as demonstrated when we compute free energy differences associated with chemical reactions in the previous works.[41,45] The detailed description for the implementation of the QM/MM-ER approach including the computation of $\delta\mu$ was given in ref 34.

III. Computational Details

Molecular geometries for the QM subsystem have been optimized by the Kohn−Sham density functional theory (KS-DFT)[48−50] employing Gaussian 03[47] at the BLYP/aug-cc-pVDZ[51−53] level of theory. As the molecular structure of acetic acid, the syn conformation has been chosen since the chemical potential of the syn conformer is more stable by 1−2 kcal/mol than that of the anti conformer.[46,54−57] To obtain the zero-point energy and vibration−rotational free energy, the frequency analysis has been performed for each solute molecule.

In the QM/MM simulations, the electronic structures for the QM solutes (CH_3COOH and CH_3COO^-) have been determined by the KS-DFT, where the one-electron wave functions have been expressed by the real-space grids.[35,58−61] The QM cell has been embedded at the center of the MM simulation cell with periodic boundary condition. The QM cell is discretized by the equally spaced 64 grids along each direction, for which the grid spacing is set at 0.287 au (0.152 Å). The fourth-order finite difference scheme has been employed to represent the kinetic energy operator. As for the nucleus−electron interactions, pseudopotentials NCPS 97[62] developed by the methods of Troullier and Martins[63] have been employed and the timesaving double grid technique proposed by Ono and Hirose[64] has been implemented to reproduce accurately the rapid behavior of the nonlocal part of the pseudopotentials near the atomic core regions. To eliminate the periodicity of the QM subsystem, Hartree potential has been computed by the method developed by Barnett et al.[65] The exchange-correlation energy for electrons has been estimated by the BLYP functional.[51,52]

The OPLS all atom force field[66] has been applied to the van der Waals interactions between the QM and the MM subsystems except for the size parameters for the carboxylate carbon and oxygens in the acetate ion. Table 1 summarizes the Lennard-Jones (LJ) parameters assigned for the QM solutes (CH_3COOH and CH_3COO^-). The size parameters for the carboxylate carbon and the carboxylate oxygens have been set at 2.636 and 2.081 Å, respectively, so as to reproduce the result of an ab initio calculation for the two-body interaction energy between the acetate ion and the water molecule. The LJ parameters between unlike atoms have been determined by the standard mixing rules such that $\sigma_{ij} = \sqrt{\sigma_{ii}\sigma_{jj}}$ and $\epsilon_{ij} = \sqrt{\epsilon_{ii}\epsilon_{jj}}$. The MM subsystem

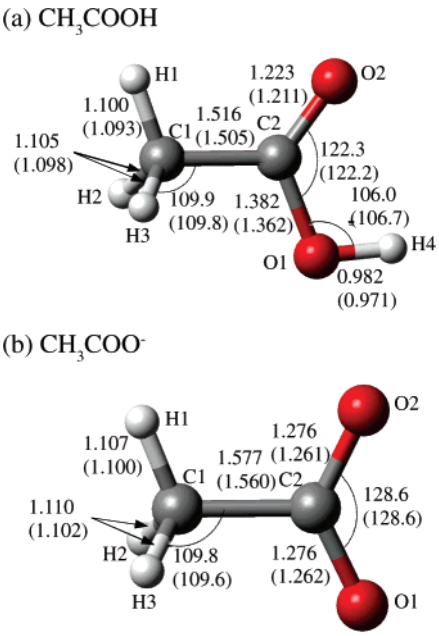

Figure 1. The molecular geometries for (a) CH_3COOH and (b) CH_3COO^- optimized by BLYP/AUG-cc-pVDZ calculations. The values in parentheses are the optimized parameters computed by the B3LYP/AUG-cc-pVDZ. Units for distances and angles are in angstroms and degrees, respectively.

consists of 253 TIP4P water molecules[67] which have been driven by the leapfrog algorithm[68] with the time step of 1 fs under the constant-*NVT* condition. The thermodynamic condition has been set at $T = 300$ K and $\rho = 1.0$ g/cm^3. The Ewald method[69] has been used to describe the long-range Coulomb interactions between water molecules.

To obtain the average distortion energy $\bar{E}$ and the average electron density $\tilde{n}(\mathbf{r})$, the 50-ps QM/MM simulation has been performed after 5-ps equilibration with the QM subsystem fixed at the structure optimized in the gas phase. Subsequently, 200- and 100-ps molecular dynamics (MD) simulations have been conducted to construct the energy distribution functions for the pure solvent and the solution system, respectively, for the solute with the average density $\tilde{n}(\mathbf{r})$. Four sets of MD simulations starting from different molecular configurations and velocities for the MM subsystem have been carried out to estimate the statistical error in the solvation free energy calculations. The energy distribution function is constructed for the solvent water molecules of which oxygen is located within the sphere of the radius 9 Å from the center of mass of the QM subsystem. For the ionic systems, the contribution due to the long-range ion−dipole interaction to the solvation free energy is estimated by the Born equation[70]

$$\mu_{\mathrm{Born}} = -16.59Z^2(1 - \epsilon^{-1})/r \qquad (23)$$

where Z, ϵ, and r are respectively the total charge of the QM subsystem in the unit of elementary charge, the dielectric constant of water at a given thermodynamic condition, and the radius of the sphere in nanometers. For the solvation free energies of the H_2O molecule and OH anion, we have employed our previous results given by the QM/MM-ER simulations.

IV. Results and Discussion

A. Gas-Phase Calculations. Parts a and b of Figure 1 show the structures for CH_3COOH and CH_3COO^- molecules optimized at the BLYP/AUG-cc-pVDZ level in the gas phase,

TABLE 2: Energy Differences ΔE_0 in Eq 11 Obtained by Employing Various Theories and Basis Sets[a]

	BLYP	B3LYP	MP4(SDTQ)	QCISD(T)	CCSD(T)
6-31G(d,p)	−66.2	−65.2	−65.1	−64.3	−64.2
cc-pVDZ	−72.1	−70.3	−71.0	−70.3	−70.1
cc-pVTZ	−60.7	−59.6	−60.5		
6-31G+(d,p)	−41.6	−42.8	−42.9	−43.3	−43.3
6-31G++(d,p)	−41.5	−42.7	−42.7	−43.1	−43.2
aug-cc-pVDZ	−39.6	−41.1	−40.2	−41.4	−41.4
aug-cc-pVTZ	−39.7	−41.4			
real-space grids	−37.8				

[a] The result given by the real-space-grid approach is also shown for comparison. The molecular geometry used is that optimized at the BLYP/AUG-cc-pVDZ level in Gaussian03. Energies are in kcal/mol.

respectively. The geometries for H_2O and OH^- molecules have also been optimized in the same manner. The angle of HOH and the bond distance for H_2O have been computed as 104.1° and 0.975 Å, respectively, while the bond length of the OH anion has been obtained as 0.981 Å. We have also performed the optimizations at the B3LYP/aug-cc-pVDZ[52,53,71] level to examine the functional dependence of the geometrical parameters and have found that there is no significant difference between the geometries determined by the BLYP and the B3LYP functionals. As a result, the energy difference ΔE_0 in eq 11 has been computed as −39.6 kcal/mol with BLYP/aug-cc-pVDZ, which is almost comparable to the value of the real-space grid approach employing the same functional (ΔE_0 = −37.8 kcal/mol). To examine the accuracy of the DFT approach, we have computed the energy differences by employing various molecular orbital (MO) theories[72] with several Gaussian basis sets. Table 2 summarizes the results obtained by MO and DFT calculations. It can be recognized in Table 2 that the energy difference ΔE_0 is significantly underestimated by the lack of the diffuse type basis. It is also shown that the DFT calculation with the B3LYP functional gives comparable accuracy in energy to the high level MO theories. The energy difference computed by B3LYP/aug-cc-pVDZ is −41.1 kcal/mol, which is in excellent agreement with that obtained by MP4(SDTQ)[73] (−40.2 kcal/mol), QCISD(T)[74] (−41.4 kcal/mol), and CCSD(T)[74,75] (−41.4 kcal/mol). We have also performed DFT calculations with a valence triples basis set (aug-cc-pVTZ basis)[53] and found that triple-split valence makes only a slight change in energetics. The valence triple-ζ basis sets (cc-pVTZ and aug-cc-pVTZ) are not available for most of the high-level MO theories in our computational environment. Thus, it has been found that the BLYP functional slightly underestimates the energy difference as compared with the B3LYP calculations in accord with a well-known trend in DFT. Hence, it is expected that the employment of the BLYP functional for the computation of ΔE_0 may cause a minor error when one computes the relative acidity.

The zero point energy E_{ZPE} and the vibrational−rotational free energy μ_{vibrot} have also been computed by the frequency analyses in Gaussian 03. The difference ΔE_{ZPE} decreases the energy difference by 0.7 kcal/mol between the product and the reactant, while the free-energy difference $\Delta\mu_{vibrot}$ has been estimated to be −1.7 kcal/mol. As a result, the free energy change ΔG_{gas} ($=\Delta E_0 + \Delta E_{ZPE} + \Delta\mu_{vibrot}$) has been obtained as −40.2 kcal/mol when we adopt the value of $\Delta E_0 = -37.8$ kcal/mol computed by the real-space grid approach with the BLYP functional.

B. QM/MM-ER Simulations in Aqueous Solution. Next we have performed the QM/MM-ER simulations to compute solvation free energies for the solutes CH_3COOH and CH_3COO^-. The ordinary QM/MM simulations have been performed to obtain the average electron density $\tilde{n}(\mathbf{r})$ and the distortion energy $\bar{E}$. Then MD simulations have been performed for the solute with the fixed electron density $\tilde{n}(\mathbf{r})$ to compute the solvation free energy $\Delta\bar{\mu}$ in eq 20.

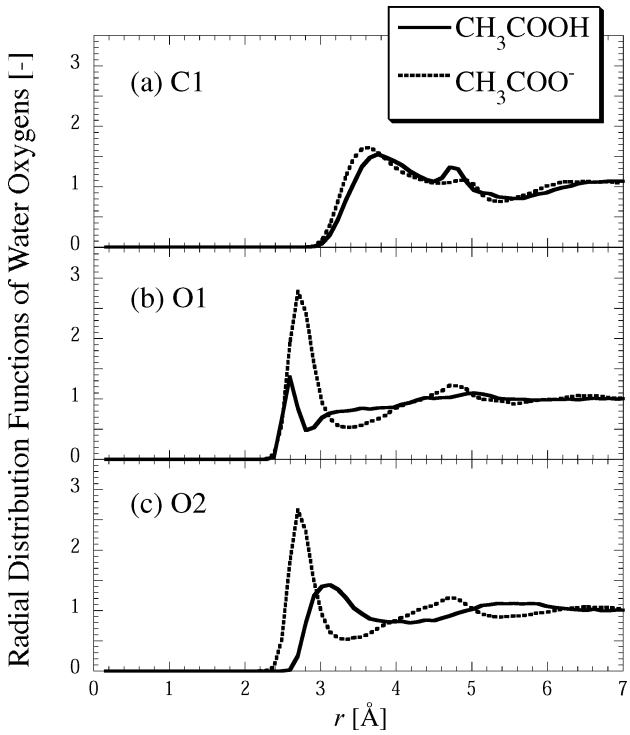

Figure 2. Radial distribution functions for water molecules around (a) C1, (b) O1, and (c) O2 atoms in CH_3COOH and CH_3COO^- molecules. The atom labels correspond to those in Figure 1.

Figures 2 show the radial distribution functions (RDFs) for the MM water oxygens around the QM atoms of interest (C1, O1, and O2 in Figure 1). In Figure 2a, there is no remarkable difference in the RDF around the C1 atom between the neutral CH_3COOH and CH_3COO anion. Only a slight change due to the deprotonation process is made around the second peak of the RDF on the C1 atom, which may correspond to the water molecule bound to the hydroxyl hydrogen H4 of the CH_3COOH solute (Figure 1a). On the other hand, a significant difference between the neutral and the anionic solutes can be recognized in the solvation structures around the O1 and O2 atoms. For the acetic acid, the RDFs around the O1 and O2 atoms show the typical hydrogen bond structures where their first peaks are positioned around 2.5 Å for O1 and 3 Å for O2. As compared with these hydration structures, the first peak of the RDFs around the COO group of the acetate anion becomes much more intensive due to the ion−dipole interaction. As can be seen in Figure 2b,c. First peaks around the O1 and O2 atoms of the CH_3COO anion are nearly two times as large as those of the acetic acid. Thus, the RDFs indicate that the proton dissociation of acetic acid accompanies the substantial solvent reorganization especially around the carboxyl group. Table 3 shows the fractional charge on each QM site for the CH_3COOH and CH_3COO anion. The instantaneous point charges have been optimized at each MD step by the least-square fittings so that they reproduce the electrostatic potential formed by the QM subsystem. Then the fractional charges have been estimated by averaging the instantaneous charges over 50 ps through the QM/MM simulations. As seen in Table 3, the total charge of the CH_3 groups has been estimated to be 0.027 for the acetic acid and 0.070 for the acetate anion. There is no remarkable difference in the charge distributions. On the other hand, the

TABLE 3: Fractional Charges for the Acetic Acid and the Acetate Ion in the Aqueous Solution in Units of Elementary Charges

	CH_3COOH	CH_3COO^-
C1	−0.4227	0.1776
H1	0.1284	−0.0456
H2	0.1530	−0.0326
H3	0.1681	−0.0293
C2	0.7720	0.7890
O1	−0.6360	−0.9409
O2	−0.6557	−0.9182
H4	0.4929	

total charge of the COOH group for the CH_3COOH has been estimated to be −0.027 and that of COO^- for the CH_3COO anion has been obtained as −1.070, indicating that the excess electron mainly localizes at the COO group of the acetate anion. It has been found that the charge distributions in the QM solutes are fully consistent with the difference in the solvation structures between acetic acid and acetate ion.

In the method of the energy representation, the spatial distribution of the solvent molecules is projected onto a one-dimensional energy coordinate defined by the solute−solvent interaction potential. The energy distribution functions $\rho(\epsilon)$ in the solution system as well as $\rho_0(\epsilon)$ in the reference system are used as inputs to eq 19. $\rho_0(\epsilon)$ gives a reference distribution with respect to the solute insertion into the solvent. Figure 3 shows the energy distribution functions for the CH_3COOH and CH_3COO^- solute. In Figure 3a, two peaks in the energy distribution functions can be found around −5 and −10 kcal/mol for the solution system. A peak around −5 kcal/mol corresponds to the single hydrogen bonds between the solute and the solvent and the other can be attributed to the water molecules that make simultaneously two hydrogen bonds with acetic acid. As for the CH_3COO anion (Figure 3b), on the other hand, one can find a notable peak on the lower energy coordinate (−13 kcal/mol), which can be attributed to the ion−dipole interaction between the solute and the solvent.

We have computed solvation free energies for CH_3COOH and CH_3COO^- solute by employing the energy distribution functions in Figure 3. Table 4 shows the solvation free energies for CH_3COOH and CH_3COO^- solutes. The solvation free energies $\Delta\bar{\mu}$ for the solute with average electron densities have been computed as −7.7 kcal/mol for CH_3COOH and −58.5 kcal/mol for CH_3COO^-. The electronic distortion energy $\bar{E}$ for CH_3COO^- (11.7 kcal/mol) is much larger than that for CH_3COOH (3.5 kcal/mol), implying that the excess charge on the acetate ion is more flexible under the influence of the electrostatic field formed by the MM water molecules. We have made the Born's correction for the anionic system to compensate the contribution outside the sphere of radius 9 Å, which has been estimated as −18.2 kcal/mol. Totally the solvation free energies have been obtained as −4.2 kcal/mol for acetic acid and −65.0 kcal/mol for acetate ion.

C. Relative Acidity of Acetic Acid. Finally, we have computed the relative acidity of the acetic acid given by eq 5 or eq 12. The QM/MM-ER simulations for the H_2O and OH^- solutes were also performed in the previous work and the solvation free energies were obtained as −5.8 and −94.4 kcal/mol, respectively. The third power of the thermal de Broglie wave length λ for each solute has been evaluated by eq 9. Table 5 summarizes the relative acidity of the acetic acid and the free energy components along with an experimental value. As has been shown in the table, the relative acidity ΔpK_a expressed as eq 12 for acetic acid has been computed as −9.1 where the translational contribution $\Lambda = [\lambda(CH_3COOH)\lambda(OH^-)]/[\lambda(CH_3COO^-)\lambda(H_2O)]$ and the free energy term $-[(\Delta G_0)/(k_BT)]$ are respectively obtained as 1.06 and 20.8. The experimental value of ΔpK_a is given as −11.0 when we adopt the values $pK_a^{CH_3COOH} = 4.76$ for acetic acid and $pK_a^{H_2O} = 15.74$ for water. As compared with the experimental result, the QM/MM-ER approach underestimates the value of ΔpK_a by ∼2.0. This is due mainly to the employment of the BLYP functional in the electronic structure calculations as discussed in section IVA. Actually, when we adopt the values of ΔE_0 given by CCSD(T)/AUG-cc-pVDZ (−41.4 kcal/mol) or B3LYP/AUG-cc-pVDZ (−41.1 kcal/mol) calculations, the relative acidities ΔpK_a are decreased to −11.7 and −11.5, respectively.

We have also performed the PCM calculations at the BLYP/aug-cc-pVDZ level to make comparisons with the present approach and have found that the PCM fails significantly to estimate the relative acidity ($\Delta pK_a = -18.6$) due to the poor description of the difference in the solvation free energies. Table 6 shows the comparison of the solvation free energies obtained by the QM/MM-ER, PCM, and experimental approaches. As has been shown in the table, the difference in the solvation free

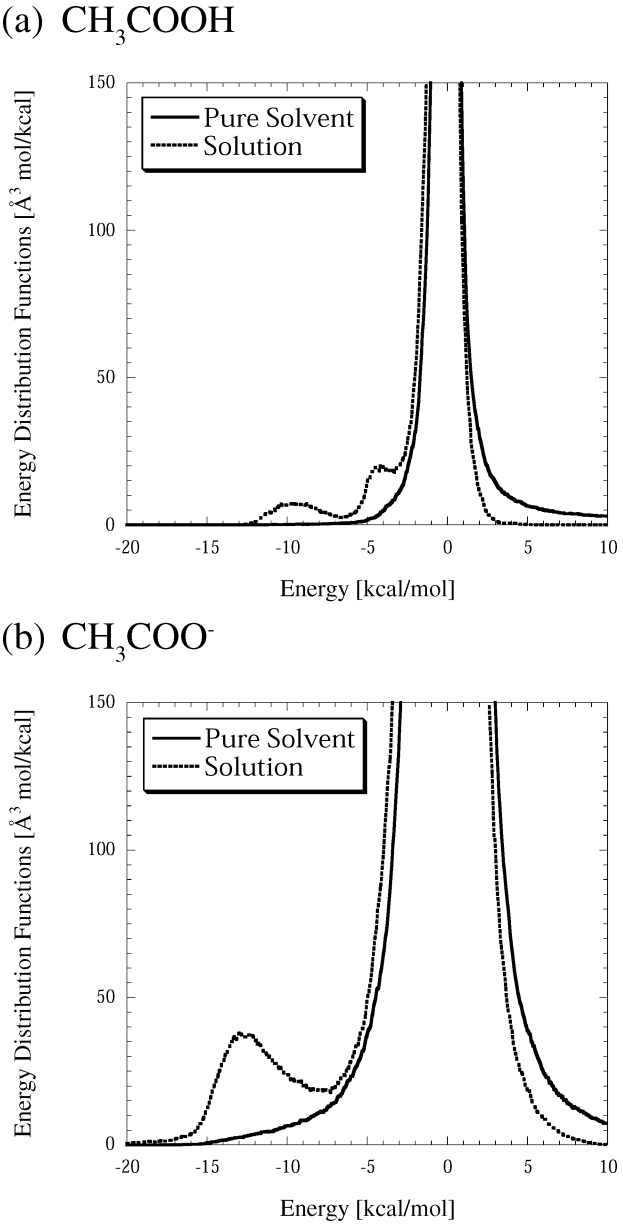

Figure 3. Energy distribution functions for (a) CH_3COOH and (b) CH_3COO^- in aqueous solution.

TABLE 4: Solvation Free Energies and Its Components for CH_3COOH and CH_3COO^- [a]

	CH_3COOH	CH_3COO^-
μ_{solv}	−4.2	−65.0
$\Delta\bar{\mu}$	−7.7(±0.5)	−58.5(±0.9)
1	−8.41	−57.86
2	−7.37	−59.78
3	−7.53	−58.18
4	−7.55	−57.98
$\bar{E}$	3.5	11.7
$\delta\mu$ [b]		
μ_{Born} [c]		−18.2

[a] The values in parentheses indicate error bars estimated from the four sets of MD simulations. The $\Delta\bar{\mu}$ obtained from each set of simulation are also shown. Energies are in kcal/mol. [b] The term δm in eq 20 has been neglected in the present work due to the minor contribution of the many-body effect to the free energy difference. [c] Born's correction of eq 23 for the anionic system has been made to compensate for the contribution of the long-range ion−dipole interactions.

TABLE 5: The Relative Acidity and the Free Energy Components in Eqs 11 and 12 Computed by the Gaussian Package and the QM/MM-ER Approach[a]

ΔpK_a(exptl)	−11.0
$pK_a^{CH_3COOH}$ [b]	4.76
$pK_a^{H_2O}$ [b]	15.74
ΔpK_a(QM/MM-ER)	−9.1
Λ [c]	1.06
ΔE_0	−37.8
ΔE_{ZPE}	−0.7
Δm_{vibrot}	−1.7
Δm_{solv}	27.8

[a] An experimental value is also shown for comparison. Energies are in the units of kcal/mol. [b] See ref 2. [c] $\Lambda = [\lambda(CH_3COOH)\lambda(OH^-)]/[\lambda(CH_3COO^-)\lambda(H_2O)]$.

TABLE 6: Comparisons of the Solvation Free Energies Computed by the PCM and QM/MM-ER Approaches. Corresponding Experimental Values Are Also Shown as References[a]

	μ_{solv}				
	CH_3COOH	OH^-	CH_3COO^-	H_2O	$\Delta\mu_{solv}$
QM/MM-ER	−4.2	−94.4	−65.0	−5.8	27.8
PCM	−3.2	−79.2	−60.7	−5.1	16.6
exptl[b]	−6.7	−105.0	−77.3	−6.3	28.1

[a] Energies are in kcal/mol. [b] See ref 2.

energies given by QM/MM-ER ($\Delta\mu_{solv}$ = 27.8 kcal/mol) between the product and the reactant is in excellent agreement with the experimental value (28.1 kcal/mol). On the other hand, the difference has been estimated to be 16.6 kcal/mol by the PCM approach, resulting from the serious underestimation of the solvation free energies on anionic solutes especially for the OH anion.

It should also be noted that the contribution of the electron density fluctuation $\delta\mu$ in eq 20 is neglected in the present work. In the previous work,[45] we found that $\delta\mu$ cannot be overlooked when one computes solvation free energies for anionic molecules. Actually the underestimation of the solvation free energies by the QM/MM-ER approach shown in Table 6 can be mainly attributed to the neglect of the electron density fluctuation. However, the contribution is always negative in energy and it weakly depends on the molecular species, and hence one can expect that cancellation of $\delta\mu$ takes place in the calculation of the free energy change associated with a reaction. In summary, it has been demonstrated that the QM/MM-ER approach is efficient and adequate for the calculation of the acidity/basicity of organic molecules in aqueous solution.

V. Conclusions

In the present work, we have utilized the methodology, referred to as QM/MM-ER, based on the ab initio QM/MM approach combined with the theory of energy representation to deal with the acidity/basicity of an organic molecule relative to water. The proton dissociation of acetic acid has been chosen as a benchmark. Adopting the free energy change in the gas phase determined by the DFT calculations with the B3LYP functional, the relative acidity has been computed as ΔpK_a = −11.5 in excellent agreement with an experimental value of −11.0. On the contrary, the employment of the reaction field based on the continuum model has failed seriously to reproduce the relative acidity. It should also be stressed that QM/MM-ER is more advantageous to the free energy calculations than the QM/MM method coupled with a numerically rigorous algorithm such as free energy perturbation or thermodynamic integration since the theory of energy representation is computationally much less costly. The QM/MM-ER approach can afford adequate energetics for chemical events in condensed systems under a modest computational environment. The extension of the approach to the biological systems is also straightforward. Work is now in progress to determine the protonation state of the active sites in enzymes.

Acknowledgment. The present work was supported by Grants-in-Aid for Scientific Research (Grant Nos. 15360422, 15-4075, and 18031022) and the Next Generation Super Computing Project, Nanoscience Program, MEXT, Japan. This work was also supported by the National Institutes of Health in the United States. T.H. thanks Dr. Hao Hu at Duke University for the fruitful discussions on his QM/MM methodology to evaluate the free energy difference in condensed systems. H.T. is grateful to Dr. N. Matubayasi at Kyoto university for valuable discussions.

References and Notes

(1) Topol, I. A.; Tawa, G. J.; Caldwell, R. A.; Eissenstat, M. A.; Burt, S. K. *J. Phys. Chem. A* **2000**, *104*, 9619−9624.
(2) Takano, Y.; Houk, K. N. *J. Chem. Theory Comput.* **2005**, *1*, 70−77.
(3) Kawata, M.; Ten-no, S.; Kato, S.; Hirata, F. *J. Am. Chem. Soc.* **1995**, *117*, 1638−1640.
(4) Kawata, M.; Ten-no, S.; Kato, S.; Hirata, F. *Chem. Phys. Lett.* **1995**, *240*, 199−204.
(5) Kawata, M.; Ten-no, S.; Kato, S.; Hirata, F. *Chem. Phys.* **1996**, *203*, 53−67.
(6) Kawata, M.; Ten-no, S.; Kato, S.; Hirata, F. *J. Phys. Chem.* **1996**, *100*, 1111−1117.
(7) Sato, H.; Hirata, F. *J. Phys. Chem. A* **1998**, *102*, 2603−2608.
(8) Sato, H.; Hirata, F. *J. Phys. Chem. B* **1999**, *103*, 6596−6604.
(9) Li, G.; Cui, Q. *J. Phys. Chem. B* **2003**, *107*, 14521−14528.
(10) Yagasaki, T.; Iwahashi, K.; Saito, S.; Ohmine, I. *J. Chem. Phys.* **2005**, *122*, 144504−144512.
(11) Gao, D.; Svoronos, P.; Wong, P. K.; Maddalena, D.; Hwang, J.; Walker, H. *J. Phys. Chem. A* **2005**, *109*, 10776−10785.
(12) Antosiewicz, J.; McCammon, J. A.; Gilson, M. K. *J. Mol. Biol.* **1994**, *238*, 415−436.
(13) Lim, C.; Bashford, D.; Karplus, M. *J. Phys. Chem.* **1991**, *95*, 5610−5620.
(14) Antosiewicz, J.; McCammon, J. A. *Biochemistry* **1996**, *35*, 7819−7833.
(15) Minikis, R. M.; Kairys, V.; Jensen, J. H. *J. Phys. Chem. A* **2001**, *105*, 3829−3837.
(16) Piana, S.; Sebastiani, D.; Carloni, P.; Parrinello, M. *J. Am. Chem. Soc.* **2001**, *123*, 8730−8737.
(17) Li, H.; Hains, A. W.; Everts, J. E.; Robertson, A. D.; Jensen, J. H. *J. Phys. Chem. B* **2002**, *106*, 3486−3494.

(18) Nakajima, S.; Ohno, K.; Inoue, Y.; Sakurai, M. *J. Phys. Chem. B* **2003**, *107*, 2867−2874.
(19) Yoda, M.; Inoue, Y.; Sakurai, M. *J. Phys. Chem. B* **2003**, *107*, 14569−14575.
(20) Simonson, T.; Carlsson, J.; Case, D. A. *J. Am. Chem. Soc.* **2004**, *126*, 4167−4180.
(21) Li, H.; Robertson, A. D.; Jensen, J. H. *Proteins*: *Struct., Funct., Bioinf.* **2004**, *55*, 689−704.
(22) Tomasi, J.; Persico, M. *Chem. Rev.* **1994**, *94*, 2027−2094.
(23) Ten-no, S.; Hirata, F.; Kato, S. *Chem. Phys. Lett.* **1993**, *214*, 391−396.
(24) Warshel, A.; Levitt, M. *J. Mol. Biol.* **1976**, *103*, 227−249.
(25) Gao, J.; Xia, X. *Science* **1992**, *258*, 631−635.
(26) Zhang, Y.; Lee, T. S.; Yang, W. *J. Chem. Phys.* **1999**,*110*, 46−54.
(27) Zhang, Y.; Liu, H.; Yang, W. *J. Chem. Phys.* **2000**,*112*, 3483−3492.
(28) Lu, Z.; Yang, W. *J. Chem. Phys.* **2004**, *121*, 89−100.
(29) Hu, H.; Yang, W. *J. Chem. Phys.* **2005**, *123*, 041102−04110.5.
(30) Cisneros, G. A.; Liu, H.; Zhang, Y.; Yang, W. *J. Am. Chem. Soc.* **2003**, *125*, 10384−10393.
(31) Cisneros, G. A.; Wang, M.; Silinski, P.; Fitzgerald, M. C.; Yang, W. *J. Phys. Chem. A* **2006**, *110*, 700−708.
(32) Formaneck, M. S.; Li, G.; Zhang, X.; Cui, Q. *J. Theor. Comput. Chem.* **2002**, *1*, 53−67.
(33) Li, G.; Zhang, X.; Cui, Q. *J. Phys. Chem. B* **2003**, *107*, 8643−8653.
(34) Takahashi, H.; Matubayasi, N.; Nakahara, M.; Nitta, T. *J. Chem. Phys.* **2004**, *121*, 3989−3999.
(35) Takahashi, H.; Hori, T.; Hashimoto, H.; Nitta, T. *J. Comput. Chem.* **2001**, *22*, 1252−1261.
(36) Hori, T.; Takahashi, H.; Nitta, T. *J. Comput. Chem.* **2003**, *24*, 209−221.
(37) Takahashi, H.; Takei, S.; Hori, T.; Nitta, T. *J. Mol. Struct.* (*Theochem*) **2003**, *632*, 185−195.
(38) Takahashi, H.; Hashimoto, H.; Nitta, T. *J. Chem. Phys.* **2003**, *119*, 7964−7971.
(39) Hori, T.; Takahashi, H.; Nitta, T. *J. Chem. Phys.* **2003**, *119*, 8492−8499.
(40) Hori, T.; Takahashi, H.; Nitta, T. *J. Theor. Comput. Chem.* **2005**, *4*, 867−882.
(41) Takahashi, H.; Kawashima, Y.; Nitta, T. *J. Chem. Phys.* **2005**, *123*, 124504−124512.
(42) Matubayasi, N.; Nakahara, M. *J. Chem. Phys.* **2000**, *113*, 6070−6081.
(43) Matubayasi, N.; Nakahara, M. *J. Chem. Phys.* **2002**, *117*, 3605−3616. Matubayasi, N.; Nakahara, M. *J. Chem. Phys.* **2003**, *118*, 2446.
(44) Matubayasi, N.; Nakahara, M. *J. Chem. Phys.* **2003**, *119*, 9686−9702.
(45) Takahashi, H.; Satou, W.; Hori, T.; Nitta, T. *J. Chem. Phys.* **2005**, *122*, 044504−044512.
(46) Hori, T.; Takahashi, H.; Nakano, M.; Nitta, T.; Yang, W. *Chem. Phys. Lett.* **2006**, *419*, 240−244.
(47) Frisch, M. J.; Trucks, G. W.; Schlegel, H. B.; Scuseria, G. E.; Robb, M. A.; Cheeseman, J. R.; Montgomery, J. A., Jr.; Vreven, T.; Kudin, K. N.; Burant, J. C.; Millam, J. M.; Iyengar, S. S.; Tomasi, J.; Barone, V.; Mennucci, B.; Cossi, M.; Scalmani, G.; Rega, N.; Petersson, G. A.; Nakatsuji, H.; Hada, M.; Ehara, M.; Toyota, K.; Fukuda, R.; Hasegawa, J.; Ishida, M.; Nakajima, T.; Honda, Y.; Kitao, O.; Nakai, H.; Klene, M.; Li, X.; Knox, J. E.; Hratchian, H. P.; Cross, J. B.; Adamo, C.; Jaramillo, J.; Gomperts, R.; Stratmann, R. E.; Yazyev, O.; Austin, A. J.; Cammi, R.; Pomelli, C.; Ochterski, J. W.; Ayala, P. Y.; Morokuma, K.; Voth, G. A.; Salvador, P.; Dannenberg, J. J.; Zakrzewski, V. G.; Dapprich, S.; Daniels, A. D.; Strain, M. C.; Farkas, O.; Malick, D. K.; Rabuck, A. D.; Raghavachari, K.; Foresman, J. B.; Ortiz, J. V.; Cui, Q.; Baboul, A. G.; Clifford, S.; Cioslowski, J.; Stefanov, B. B.; Liu, G.; Liashenko, A.; Piskorz, P.; Komaromi, I.; Martin, R. L.; Fox, D. J.; Keith, T.; Al-Laham, M. A.; Peng, C. Y.; Nanayakkara, A.; Challacombe, M.; Gill, P. M. W.; Johnson, B.; Chen, W.; Wong, M. W.; Gonzalez, C.; Pople, J. A. *Gaussian 03*, Revision B.05; Gaussian, Inc.: Pittsburgh, PA, 2003.
(48) Hohenberg, P.; Kohn, W. *Phys. Rev.* **1964**, *136*, B864−871.
(49) Kohn, W.; Sham, L. *J. Phys. Rev.* **1965**, *140*, A1133−1138.
(50) Parr, R. G.; Yang, W. *Density-Functional Theory of Atoms and Molecules*; Oxford University Press: New York, 1989.
(51) Becke, A. D. *Phys. Rev. A* **1988**, *38*, 3098−3100.
(52) Lee, C.; Yang, W.; Parr, R. G. *Phys. Rev. B* **1988**, *37*, 785−789.
(53) Dunning, T. H., Jr. *J. Chem. Phys.* **1989**, *90*, 1007−1023.
(54) Gao, J.; Pavelites, J. J. *J. Am. Chem. Soc.* **1992**, *114*, 1912−1914.
(55) Sato, H.; Hirata, F. *J. Mol. Struct.* (*Theochem*) **1999**, *461*−*462*, 113−120.
(56) Huff, J. B.; Askew, B.; Duff, R. J.; Rebek, J., Jr. *J. Am. Chem. Soc.* **1988**, *110*, 5908−5909.
(57) Tadayoni, B. M.; Parris, K.; Rebek, J., Jr. *J. Am. Chem. Soc.* **1989**, *111*, 4503−4505.
(58) Chelikowsky, J. R.; Troullier, N.; Saad, Y. *Phys. Rev. Lett.* **1994**, *72*, 1240−1243.
(59) Chelikowsky, J. R.; Troullier, N.; Wu, K.; Saad, Y. *Phys. Rev. B* **1994**, *50*, 11355−11364.
(60) Jing, X.; Troullier, N.; Dean, D.; Binggeli, N.; Chelikowsky, J. R.; Wu, K.; Saad, Y. *Phys. Rev. B* **1994**, *50*, 12234−12237.
(61) Takahashi, H.; Hori, T.; Wakabayashi, T.; Nitta, T. *J. Phys. Chem. A* **2001**, *105*, 4351−4358.
(62) Kobayashi, K. *Comput. Mater. Sci.* **1999**, *14*, 72−76.
(63) Troullier, N.; Martins, J. L. *Phys. Rev. B* **1991**, *43*, 1993−2006.
(64) Ono, T.; Hirose, K. *Phys. Rev. Lett.* **1999**, *82*, 5016−5019.
(65) Barnett, R. N.; Landman, U. *Phys. Rev. B* **1993**, *48*, 2081−2097.
(66) Jorgensen, W. L.; Maxwell, D. S.; Tirado-Rives, J. *J. Am. Chem. Soc.* **1996**, *118*, 11225−11236.
(67) Jorgensen, W. L.; Chandrasekhar, J.; Madura, J. D.; Impey, R. W.; Klein, M. L. *J. Chem. Phys.* **1983**, *79*, 926−935.
(68) Allen, M. P.; Tildesley, D. J. *Computer Simulation of Liquids*; Oxford University Press: Oxford, UK, 1987.
(69) Ewald, P. *Ann. Phys.* (*Paris*, *Fr.*) **1921**, *64*, 253−287.
(70) Born, M. *Z. Phys.* **1920**, *1*, 45−48.
(71) Becke, A. D. *J. Chem. Phys.* **1993**, *98*, 5648−5652.
(72) Szabo, A.; Ostlund, N. S. *Modern Quatum Chemistry*; Macmillan: New York, 1982.
(73) Krishnan, R.; Pople, J. A. *Int. J. Quantum Chem.* **1978**, *14*, 91−100.
(74) Pople, J. A.; Head-Gordon, M.; Raghavachari, K. *J. Chem. Phys.* **1987**, *87*, 5968−5975.
(75) Purvis, G. D., III; Bartlett, R. J. *J. Chem. Phys.* **1982**, *76*, 1910−1918.